Published in final edited form as:
Am J Ophthalmol. 2015 February ; 159(2): 393–403.e2. doi:10.1016/j.ajo.2014.11.010.

Advanced Imaging for Glaucoma Study: Design, Baseline Characteristics, and Inter-Site Comparison

Phuc V. Le[1], **Xinbo Zhang**[2], **Brian A. Francis**[3,*], **Rohit Varma**[1], **David S. Greenfield**[4], **Joel S. Schuman**[5], **Nils Loewen**[5], **David Huang**[2], and **on behalf of the Advanced Imaging for Glaucoma Study Group**[6]

[1]Department of Ophthalmology, University of Southern California, Los Angeles, CA, USA

[2]Casey Eye Institute, Oregon Health & Science University, Portland, OR, USA

[3]Doheny Eye Institute, University of Southern California, Los Angeles, CA, USA

[4]Bascom Palmer Eye Institute, University of Miami, Miami, FL, USA

[5]Eye and Ear Institute, University of Pittsburgh Medical Center, Pittsburgh, PA, USA

Abstract

Purpose—To report the baseline characteristics of the participants in the Advanced Imaging for Glaucoma Study. To compare the participating sites for variations among subjects and the performance of imaging instruments.

Design—Multi-center longitudinal observational cohort study

Methods—A total of 788 participants (1,329 eyes) were enrolled from three academic referral centers. There were 145 participants (289 eyes) in the normal group, 394 participants (663 eyes) in the glaucoma suspect/preperimetric glaucoma group, and 249 participants (377 eyes) in the perimetric glaucoma group.

Participants underwent a full clinical exam, standard automated perimetry, and imaging with time-domain and Fourier-domain optical coherence tomography (OCT), scanning laser polarimetry, and confocal scanning laser ophthalmoscopy.

Corresponding Author: David Huang, MD, PhD Casey Eye Institute, Oregon Health & Science University 3375 S.W. Terwilliger Blvd Portland OR 97239-4197 davidhuang@alum.mit.edu 503-494-5131.
[6]The Advanced Imaging for Glaucoma Study Group roster is listed in the Appendix.
[*]Brian A. Francis is currently at the Doheny Eye Institute, University of California, Los Angeles, CA, USA

C. Contributions of authors: Design of the study (BAF, DH, JSS, RV); conduct of the study (BAF, DH, JSS, RV); collection of the data (BAF, DSG, JSS, NAL, RV, XZ); management of the data (BAF,DSG, DH, JSS, XZ); analysis of the data (BAF, DH, JSS, NAL, PVL, RV, XZ); interpretation of the data (BAF, DH, JSS, NAL, PVL, RV, XZ); preparation of the manuscript (BAF, DSG, DH, PVL); review of the manuscript (BAF, DSG, DH, JSS, NAL, PVL, RV); approval of the manuscript (BAF, DSG, DH, JSS, NAL, PVL, RV, XZ).

All authors have completed and submitted the ICMJE form for disclosure of potential conflicts of interest.

Main Outcome Measures—The baseline average, population standard deviation, and repeatability of imaging-derived anatomic variables were reported for each technology and center.

Results—Compared to the normal participants, glaucoma suspect/preperimetric glaucoma and perimetric glaucoma groups had significantly reduced anatomic measurements. Repeatability of nerve fiber layer thickness was best for Fourier-domain OCT (overall coefficient of variation < 2%), followed by time-domain OCT (coefficient of variation 2-2.9%), scanning laser polarimetry (coefficient of variation 2.6-4.5%), and confocal scanning laser ophthalmoscopy rim area (coefficient of variation 4.2-7.6%). A mixed-effects model showed that the differences between sites was less than 25 percent of the variation within groups and less than the differences between the normal and glaucoma suspect/preperimetric glaucoma group.

Conclusions—Site-to-site variation was smaller than both the variation within groups and the changes due to glaucoma. Therefore pooling of participants between sites is appropriate.

Introduction

Glaucoma is the leading cause of irreversible blindness in the world. It has been estimated that by 2020, almost 80 million people worldwide will be afflicted with open angle glaucoma or angle closure glaucoma.[1] The diagnosis of glaucoma generally requires clinically documented changes to the optic nerve head and is often characterized by corresponding visual field defects on standard automated perimetry. However, the clinical evaluation of the optic nerve head is subjective and there is significant variability between clinicians. Moreover, clinically detectable nerve fiber layer loss can occur before reproducible defects can be seen on standard automated perimetry.[2] After being diagnosed with glaucoma, the management of patients also depends on detecting changes in the optic nerve head appearance or in the visual field, which are limited by the subjective nature of optic nerve head examination and the low reliability of visual field testing. Finally, there is an even larger population of “glaucoma suspects” and patients with “preperimetric glaucoma” that is comprised of patients with ocular hypertension, cup-to-disc asymmetry or enlarged cups, or thinning of the neuroretinal rim, but without firm evidence of glaucomatous damage to the optic nerve on standard automated perimetry.[3] Using standard automated perimetry and optic nerve exam, it can be difficult to differentiate these from early glaucoma damage, and also to determine the point at which a patient “converts” from being a glaucoma suspect to an early glaucoma patient.

Several different technologies have become available to image the optic nerve head, peripapillary retinal nerve fiber layer, and macular ganglion cell complex. These include confocal scanning laser ophthalmoscopy, scanning laser polarimetry, and optical coherence tomography (OCT). The use of these imaging technologies in glaucoma has recently been reviewed.[4-6] A few studies have compared the performance of all these technologies on the same set of participants, and have generally shown their performance to be similar.[7-11] However, most of these studies have been cross-sectional, not longitudinal, and did not include glaucoma suspects. Thus it remains unclear which imaging technology and parameters are most predictive of conversion from glaucoma suspect to perimetric glaucoma.

The goal of the Advanced Imaging for Glaucoma (AIG) Study was to develop and assess advanced imaging technologies to improve the diagnosis and management of patients with glaucoma. A similar study, the Diagnostic Innovations in Glaucoma Study (DIGS), also longitudinally evaluated several advanced imaging technologies on patients at risk for glaucoma or with glaucoma who were recruited from a single study site.[12, 13] However, the AIG Study is the first multi-center, prospective, longitudinal study designed to evaluate the four most commonly used technologies, i.e., time-domain OCT, Fourier-domain OCT, scanning laser polarimetry, and confocal scanning laser ophthalmoscopy, on eyes categorized as normal, glaucoma suspect/preperimetric glaucoma, and perimetric glaucoma. This article describes the design of the AIG Study and the baseline characteristics of the participants who have completed the enrollment process. The baseline results of the primary anatomic variables measured by the advanced imaging modalities are described in their basic forms and the validity of pooling data from multiple sites is investigated.

Methods

The AIG Study is a multi-center, longitudinal, observational cohort study. Participants were recruited at the AIG clinical centers at the University of Pittsburgh, the University of Miami, and the University of Southern California. The study protocols for the clinical centers were approved by the Institutional Review Boards at the University of Pittsburgh, the University of Miami, and the University of Southern California, respectively. The chair and coordinating center protocol was approved by the Institutional Review Board at Oregon Health & Science University. Signed informed consent as outlined in the study protocol was obtained for all participants. The study was conducted in accordance with the ethical standards as stated in the Declaration of Helsinki and the Health Insurance Portability and Accountability Act of 1996. A detailed description of our methods is provided in the AIG Study Manual of Procedures posted on the study website www.AIGStudy.net. The AIG Study is registered with www.clinicaltrials.gov (NCT01314326).

Visits and Procedures

Participants enrolled in the study had an initial qualifying visit that included obtaining a medical and ophthalmic history, eye exam (refraction, visual acuity, external and slit-lamp exam, dilated fundus exam, Goldmann applanation tonometry, pachymetry, gonioscopy), and visual field testing. During this visit, participants indicated their race by selecting from among the following choices: American Indian/Alaska Native, Asian, Native Hawaiian or Pacific Islander, Black or African American, and White. Ethnicity was indicated by selecting between Hispanic/Latino and non-Hispanic/Latino. Qualified participants then had a baseline visit during which the advanced imaging technology scans, axial eye length measurement, and stereo optic disc photography were performed. Subsequent follow-up visits were scheduled every six months for perimetric glaucoma and glaucoma suspect/preperimetric glaucoma groups, and every twelve months for the normal group. At all follow-up visits, interval history, eye exam, and advanced imaging scans were obtained. In the perimetric glaucoma and glaucoma suspect/preperimetric glaucoma groups, visual fields were tested every 6 months, and dilated disc photos were taken every 12 months. In the

normal group, visual field testing was performed and disc photographs were taken at the final or Year 4 follow-up visit, whichever was earlier.

The visual field was assessed by standard automated perimetry on the Humphrey Field Analyzer (HFA II, Carl Zeiss Meditec, Inc., Dublin, CA, USA) using the Swedish Interactive Thresholding Algorithm 24-2. The minimum requirement for reliability included less than 15% fixation losses, less than 33% false positives, and less than 33% false negatives.

Eligibility

Participants in the normal group were required to have both eyes meet the following criteria: normal visual field, intraocular pressure (IOP) less than 21 mmHg, central corneal thickness greater than 500 m, open anterior chamber angle, normal appearing optic nerve head and nerve fiber layer, and no history of glaucoma, retinal pathology, keratorefractive surgery, or chronic ocular or systemic steroid use. Normal visual fields had a normal mean deviation (MD; $P>0.05$), pattern standard deviation (PSD; $P>0.05$), and glaucoma hemifield test (GHT; 'Within Normal Limits'). Eyes categorized into the perimetric glaucoma group had glaucomatous visual field loss, defined as either abnormal PSD ($P<0.05$) or GHT ('Outside Normal Limits') in a consistent pattern on both qualifying visual field exams. They also had an optic nerve head or nerve fiber layer defect visible on slit-lamp biomicroscopy appearing as a diffuse or localized thinning of the rim, a splinter hemorrhage, a notch in the rim, or a vertical cup-to-disc ratio more than 0.2 greater than the fellow eye. Borderline visual fields met neither normal nor perimetric glaucoma criteria. The eyes categorized as glaucoma suspect had normal or borderline visual fields and either ocular hypertension (IOP ≥ 22 mmHg) or the fellow eye met the eligibility criteria for the perimetric glaucoma group. Preperimetric glaucoma was defined as having a normal or borderline visual field, but with an optic nerve head or nerve fiber layer defect as described for the perimetric glaucoma group.

Exclusion criteria for the entire study consisted of best-corrected visual acuity worse than 20/40, age < 40 or > 79 years at entry, refractive error ≥ +3 or < -7 diopters (D), previous intraocular surgery except for uncomplicated cataract extraction with posterior chamber intraocular lens insertion, diabetic retinopathy, other diseases which may cause visual field loss or optic nerve head abnormalities, inability to view or photograph the optic discs due to media opacity or poor dilation, inability to obtain advanced imaging data with acceptable quality, inability to perform reliably on automated visual field testing, life-threatening illness, and refusal of informed consent or commitment to the full-length of the study.

Endpoints

The endpoint for the normal and glaucoma suspect/preperimetric glaucoma group was the development of visual field abnormality meeting the perimetric glaucoma criteria stated above and confirmed on 3 consecutive tests. The endpoint for the perimetric glaucoma group was confirmed visual field progression on the Glaucoma Progression Analysis software installed on the Humphrey Field Analyzer II. Progression was defined as a significant change detected in at least 3 points, repeated in the same location in 3

consecutive follow-up tests, and categorized by the Glaucoma Progression Analysis software as “Likely Progression.”

Imaging Protocols

Four advanced imaging technologies were used. For time-domain OCT (Stratus OCT; Carl Zeiss Meditec, Inc., Dublin, CA, USA), the Fast Macular Thickness Map scan setting was used to scan the macula, and the Fast RNFL Thickness scan setting was used to measure the peripapillary nerve fiber layer. If the Signal Strength parameter was below 8, another scan was performed. The minimum acceptable Signal Strength parameter was 6. Images were processed with Stratus software version 4.0.

For the Fourier-domain OCT (RTVue; Optovue, Inc., Fremont, CA, USA), the ganglion cell complex scan setting was used to scan the macula, while the optic nerve head and 3-D Disc scans were used to map the optic nerve head and nerve fiber layer. Only scans with a signal strength index parameter of ≥30 were saved. Optic nerve head scans with signal strength index > 37 and ganglion cell complex scans with signal strength index > 42 were analyzed. Images were processed with RTVue software version 6.12.0.24. Fourier-domain OCT technology was introduced in 2007 to the AIG Study. Therefore it was not available at the baseline visit for some participants. In these instances, the first Fourier-domain OCT measurements were used as baseline values.

The scanning laser polarimetry device (GDx-VCC; Laser Diagnostic Technologies, San Diego, CA, USA, later acquired by Carl Zeiss Meditec, Inc, Dublin, CA, USA.) was first calibrated for corneal birefringence at baseline, and then used to perform three sets of nerve fiber layer imaging at each visit. The enhanced corneal compensation (ECC) software version 6.0.0 was used. The scans were required to have a scan quality score (Q) of 8-10.

The confocal scanning laser ophthalmoscopy images were acquired with the Heidelberg Retina Tomograph II (HRT II, Heidelberg Engineering, Heidelberg, Germany). Two optic nerve head scans were performed at each visit. The images were assessed for quality, such as the presence of eye movement, and then the optic disc margin was defined manually. All measurements were processed with HRT II software version 1.7.

Sample Size and Statistical Power

Based on previous work,[14] we assumed that the area under the receiver operator curve for each advanced imaging technology would be in the range of 0.8 to 0.9. The statistical power calculation then yielded a target of 175 participants in the perimetric glaucoma group and 170 age-matched normal participants to be able to determine the area under the receiver operator curve within ±0.06 with at least 95% confidence. For the longitudinal study of visual field conversion in glaucoma suspect/preperimetric glaucoma group participants, we assumed an overall conversion rate of 4.4% over 5 years based on the Ocular Hypertension Treatment Study.[15] Assuming that 15% of the glaucoma suspect/preperimetric glaucoma group eyes will have abnormal advanced imaging at baseline, the power calculation resulted in a target of 320 participants to detect a difference with 92% power (one-sided t-test with $p<0.05$). These calculations assumed the two eyes of each participant were perfectly

correlated and that the actual statistical power would be higher because only partial correlation exists between the two eyes.

The repeatability of advanced-imaging derived anatomic variables was assessed by coefficient of variation and intraclass correlation coefficient.[16] Generalized estimating equations were utilized to correct for the correlation between eyes within the same participant.[17] The level of statistical significance was set at $p<0.05$. The statistical analyses were performed using SAS 9.2 software (SAS Institute, Cary, NC, USA).

Results

Baseline Participant Characteristics

A total of 788 participants were enrolled. There were 145 participants (289 eyes) in the normal group, 394 participants (663 eyes) in the glaucoma suspect/preperimetric glaucoma group, and 249 participants (377 eyes) in the perimetric glaucoma group (Table 1). The participants in the normal group were significantly younger ($p<0.001$), less likely to have a family history of glaucoma ($p<0.001$), and less likely to have systemic hypertension ($p=0.011$). A great majority of the participants were white, followed by the Black/African American category. The other racial categories constituted 5.5-10.4% of the groups. The 3 clinical centers contributed evenly to enrollment, but had significant inter-site variation in age, gender, and racial composition (Table 1). Specifically the University of Pittsburgh site had younger normal subjects and more glaucoma suspect/preperimetric glaucoma and perimetric glaucoma participants of African ancestry, while the University of Southern California site had a lower percentage of female patients in the glaucoma suspect/ preperimetric glaucoma group. There were no significant differences in gender, race, or history of diabetes mellitus between any of the groups.

There were many significant differences between normal and glaucomatous eyes (Table 2) that generally followed disease severity, e.g., perimetric glaucoma eyes were more severely affected than glaucoma suspect/preperimetric glaucoma eyes. Glaucomatous eyes generally had longer axial length, thinner central corneal thickness, worse visual field, and greater cup-to-disc ratio. The baseline IOP of the glaucoma suspect/preperimetric glaucoma group was significantly higher than the other two groups due to the inclusion of participants with ocular hypertension.

The distribution of disease severity (Figure 1) was assessed by the enhanced Glaucoma Staging System 2, a glaucoma staging system based on visual field MD and PSD.[18] Almost all eyes in the normal group and most of the eyes in the glaucoma suspect/preperimetric glaucoma group were classified as either stage 0 or borderline stage. There were 10 eyes (3.5%) in the normal group that were classified as Stage 1 due to abnormal visual field MD. Abnormal visual field MD was not part of the AIG Study visual field criteria because MD can be affected by cataract and other common causes of visual loss not specific to glaucoma. Twelve eyes (3.2%) in the perimetric glaucoma group were classified as Stage 0 or borderline. These eyes had normal visual field MD values but had consistent focal visual field damage detected by GHT, which was part of the AIG Study visual field criteria. Most

of the perimetric glaucoma group had mild to moderate visual field loss, with less than 20% in the late stages (Stages 4 and 5).

In the glaucoma suspect/preperimetric glaucoma group, the majority of eyes (494 of 663 eyes, 74.5%) belonged in the preperimetric glaucoma subgroup (Figure 2). In the glaucoma suspect subgroup (169 of 663 eyes, 25.5%), most were enrolled due to ocular hypertension, while others were enrolled for the presence of perimetric glaucoma in the other eye of the same individual. At the baseline visit, most perimetric glaucoma participants were using topical glaucoma medications (Figure 3). The number of topical medications used among perimetric glaucoma eyes (1.2 ± 1.1; mean ± standard deviation) was more than those among the glaucoma suspect/preperimetric glaucoma eyes (0.4 ± 0.7).

Baseline Advanced Imaging Measurements

The primary diagnostic anatomic variables (nerve fiber layer, ganglion cell complex, and disc) from the 4 advanced imaging modalities all had significantly lower values in both glaucoma suspect/preperimetric glaucoma and perimetric glaucoma groups compared to the normals, even after the conservative Bonferroni correction (Table 3). As expected, the values were smaller in perimetric glaucoma eyes compared to the glaucoma suspect/ preperimetric glaucoma eyes.

The imaging parameters were then analyzed by study site (Table 4). In the normal group, the nerve fiber layer thicknesses as measured by both the time domain-OCT and Fourier-domain OCT variables were statistically equivalent at the 3 sites. However, the variables for the other two devices were significantly different, and in an inconsistent pattern. The University of Southern California site had significantly greater confocal scanning laser ophthalmoscopy rim area, while the University of Miami site had significantly lower scanning laser polarimetry nerve fiber layer thickness (this overall value is called TSNIT average on the scanning laser polarimetry printout). In the glaucoma suspect/preperimetric glaucoma group, there was again a significantly greater confocal scanning laser ophthalmoscopy rim area for subjects at the University of Southern California site and a trend for lower scanning laser polarimetry nerve fiber layer thickness at the University of Miami site, while the OCT nerve fiber thickness variables were statistically equivalent at all sites. In the perimetric glaucoma group, there were significant differences between the sites for all advanced imaging technologies in a consistent pattern, i.e., perimetric glaucoma patients from the University of Pittsburgh site had milder glaucoma than the other two sites.

Advanced Imaging Repeatability

A comparison of repeatability, as assessed by coefficient of variation and intraclass correlation coefficient (Table 5) showed that the best results were for Fourier-domain OCT nerve fiber layer and ganglion cell complex, followed closely by time-domain OCT nerve fiber layer. The coefficient of variation for the confocal scanning laser ophthalmoscopy rim area was worse than for the scanning laser polarimetry nerve fiber layer, but the intraclass correlation coefficient was better. The confocal scanning laser ophthalmoscopy nerve fiber layer had the worst repeatability. These patterns were consistent in all groups and sites. A

comparison between sites showed consistent performance among all 3 sites for all imaging modalities.

Putting Inter-Site Variation in Perspective

We used mixed-effects modeling to determine the relative contribution of glaucoma status, as a fixed effect, against random variations between eyes (left v. right), participants (within glaucoma diagnostic groupings), and study site (Table 6). For all imaging-derived anatomic variables, the study site was the smallest of all the effects modeled, followed by inter-eye differences. The inter-site variation was generally one fourth or less compared to the inter-participant variation. The inter-site variation was generally one half or less compared to the fixed effect of glaucoma suspect/preperimetric glaucoma status, with the exception of scanning laser polarimetry nerve fiber layer where the inter-site variation was only slightly smaller than the glaucoma suspect/preperimetric glaucoma status effect. The inter-participant variation was generally of the same magnitude as the difference between glaucoma suspect/preperimetric glaucoma and normal subjects, and smaller than the difference between perimetric glaucoma and normal subjects.

Discussion

The AIG Study has completed recruitment of normal, glaucoma suspect/preperimetric glaucoma, and perimetric glaucoma participants, and this article describes their baseline characteristics. The comparison of diagnostic accuracy, importance of image quality standards, and the results of the longitudinal study on glaucoma conversion and progression will be presented in subsequent publications.

The within-visit repeatability analysis for nerve fiber layer measurements showed that Fourier-domain OCT had the lowest coefficient of variation, followed by time-domain OCT, scanning laser polarimetry, and confocal scanning laser ophthalmoscopy. These results match previously published reports. In an early study of scanning laser polarimetry, Zangwill et al. found the coefficient of variation for average retardation, from which nerve fiber layer thickness was calculated, to be 4.2%.[19] Garas and colleagues reported coefficient of variations for overall average nerve fiber layer thickness of 2.11% and 3.22% for Fourier-domain OCT and scanning laser polarimetry (GDx-ECC), respectively.[20] For confocal scanning laser ophthalmoscopy, Sihota et al. reported a coefficient of variation of 6.24% for HRT II rim area and 12.2% for nerve fiber layer thickness.[21] These published results are consistent with ours. In addition to nerve fiber layer thickness, Fourier-domain OCT is able to measure ganglion cell complex thickness, which is even more repeatable than nerve fiber layer thickness on an overall basis. These results suggest that Fourier-domain OCT may have an advantage in the more accurate detection of glaucoma progression. This awaits assessment in the analysis of AIG Study longitudinal data.

Although confocal scanning laser ophthalmoscopy has poor repeatability in measuring nerve fiber layer thickness, it is more precise in measuring rim area. Strouthidis and colleagues also showed that rim area was one of the most repeatable confocal scanning laser ophthalmoscopy variables, and that confocal scanning laser ophthalmoscopy nerve fiber layer thickness had a coefficient of variation that was several-fold larger.[22] Thus for

confocal scanning laser ophthalmoscopy, the rim area appears to be a better anatomic variable for diagnosing and monitoring for progression of glaucoma.

A concern in pooling participants from different study sites was that the specific imaging machine and/or operators may differ in performance, thus introducing site-specific bias or increasing the overall variability. This is a concern for multi-center studies such as ours, as well as the Ocular Hypertensive Treatment Study and the European Glaucoma Prevention Study, both of which performed an ancillary study using confocal scanning laser ophthalmoscopy to measure optic nerve parameters. [23-25] While both of those studies collected imaging data from multiple centers, our study is the first to report results of analyses of inter-site variability and its magnitude in relation to other variables such as diagnostic group. For both OCT technologies, the variability between sites was very small and statistically insignificant, demonstrating that the calibrations and operations were consistent among all 3 clinical centers. For confocal scanning laser ophthalmoscopy and scanning laser polarimetry, however, there were statistically significant differences in the average measurements in the normal group. For confocal scanning laser ophthalmoscopy it is probable that the difference was due to variability in the manual drawing of the disc boundary by the operator, resulting in variation in disc and rim areas. This could affect the diagnostic accuracy of confocal scanning laser ophthalmoscopy rim area but should have less of an effect on progression analysis because the disc boundary detection is automated in follow-up scans. For scanning laser polarimetry, we do not have information to determine if the inter-site variation was due to machine, operator, or inherent variation in the normal participants. A possible explanation for scanning laser polarimetry's larger inter-site variability is the effect of atypical birefringence pattern, the incidence of which varies with age and the level of fundus pigmentation.[27-29] This could affect the scanning laser polarimetry results at the University of Miami (Palm Beach) site, where normal participants were older on average and more likely to be white. Although the ECC algorithm reduces the incidence and severity of atypical birefringence patterns, it does not completely eliminate this problem.

The mixed-effects model analysis showed that the inter-site variation was negligible compared to the disease effect and inter-individual variations for time-domain OCT, Fourier-domain OCT, and confocal scanning laser ophthalmoscopy. Thus pooling of data from multiple sites should not affect the assessment of diagnostic accuracy. This suggests that for these technologies, AIG Study results can be generalized, and normative data from a few machines can be applied to other machines in clinical use. For scanning laser polarimetry nerve fiber layer measurement, there may be inter-site variation that is not negligible compared to the glaucoma effect at the glaucoma suspect/preperimetric glaucoma level, but is negligible compared to the level of nerve fiber layer loss in the perimetric glaucoma group.

Previous cross-sectional studies have assessed the ability of these advanced imaging technologies to discriminate between normal eyes and eyes with perimetric glaucoma in the same set of participants. Zangwill et al. compared the performance of scanning laser polarimetry, confocal scanning laser ophthalmoscopy, and time-domain OCT and showed that the best variables of each technology performed similarly at detecting early to moderate

glaucoma.[7] Greaney et al. compared time-domain OCT, scanning laser polarimetry, and confocal scanning laser ophthalmoscopy to expert assessments of stereo disc photographs.[8] They found that the best individual advanced imaging variables did not perform better than disc photography grading by a panel of experts and that a combination of variables from all 3 modalities performed better than the best variables of any single modality. Medeiros et al. also compared time-domain OCT, scanning laser polarimetry, and confocal scanning laser ophthalmoscopy and found that no single technology significantly outperformed the others, but that the performance of confocal scanning laser ophthalmoscopy may be poorer than scanning laser polarimetry or OCT.[9] In another study, Kanamori et al. similarly found that time-domain OCT and scanning laser polarimetry may be better than confocal scanning laser ophthalmoscopy at discriminating eyes with mild glaucoma from normal eyes, but also that the technologies were complementary.[10] Windisch and colleagues evaluated the ability of OCT, scanning laser polarimetry, and confocal scanning laser ophthalmoscopy to detect localized nerve fiber layer defects seen on color photographs.[30] They found that scanning laser polarimetry had a higher proportion of correctly identified defects, but also had a higher number of false-positive results. Taken as a whole, the previous works suggest that advanced imaging technologies can be useful in diagnosing and managing glaucoma but that confocal scanning laser ophthalmoscopy may have poorer performance than scanning laser polarimetry and OCT. However, it also suggests that the topographic measures produced by confocal scanning laser ophthalmoscopy may be complementary to the nerve fiber layer measures produced by scanning laser polarimetry and OCT. The AIG Study will be able to compare these imaging modalities again, with updated software. In particular, the new ECC algorithm on scanning laser polarimetry may reduce the false positive results noted in previous studies. The AIG Study also included the newer Fourier-domain OCT technology, which is able to assess 3 anatomic regions - nerve fiber layer, ganglion cell complex, and optic nerve head. The development of macular ganglion cell complex assessment with Fourier-domain OCT was one of the technological accomplishments funded by the AIG Study grant.[31-33]

The AIG Study design is unusual in the longitudinal follow up of normal participants. This allows for the evaluation of age-related changes over time for imaging-derived anatomic variables. As pointed out by Leung and colleagues, it is important that these changes be calculated from longitudinal data because the rate of age-related loss in the nerve fiber layer and other structures could be different than estimates obtained from cross-sectional studies.[34, 35]

In the AIG Study, the medical treatment was not randomly assigned. Therefore the effects of IOP and medical treatment could not be independently assessed. However, the advanced imaging results were masked from the treating clinicians until the conversion or progression endpoints were reached. Therefore the clinician's decisions were not affected by the imaging results. This minimized possible bias in evaluating the power of imaging-derived measurement in the prediction of conversion and progression.

In summary, there was a significant difference between normal, glaucoma suspect/ preperimetric glaucoma, and perimetric glaucoma groups in all of the measured diagnostic variables. The repeatability of nerve fiber layer measurement was best for Fourier-domain

OCT, followed by time-domain OCT, scanning laser polarimetry, and confocal scanning laser ophthalmoscopy. The optic disc topography values for confocal scanning laser ophthalmoscopy were better than its nerve fiber layer measures, and the repeatability of confocal scanning laser ophthalmoscopy rim area was comparable to nerve fiber layer measures of the other devices. The inter-site comparison showed that the data for groups gathered at different study sites were comparable, with the possible exception of small variations in scanning laser polarimetry and confocal scanning laser ophthalmoscopy measurements. This suggests that results from this and other multi-center studies using glaucoma imaging technologies can be applied to the general population.

Acknowledgements

A. Funding Support: Supported by NIH grants: EY013516, P30-EY008098, K08EY022737; Eye and Ear Foundation (Pittsburgh, PA, USA); Research to Prevent Blindness (New York, NY, USA).

B. Financial Disclosures: Dr. Greenfield receives research support from Optovue Inc. (Fremont, CA, USA), Carl Zeiss Meditec, Inc (Dublin, CA, USA), and Heidelberg Engineering (Heidelberg, Germany). Drs. Huang and Schuman receive royalties for an optical coherence tomography patent owned and licensed by the Massachusetts Institute of Technology and Massachusetts Eye & Ear Infirmary to Carl Zeiss Meditec, Inc. (Dublin, CA, USA). Dr. Huang has a significant financial interest in Optovue, Inc. (Fremont, CA, USA), a company that may have a commercial interest in the results of this research and technology. These potential conflicts of interest have been reviewed and managed by Oregon Health & Science University. Dr. Varma has received research grants, honoraria and/or travel support from Carl Zeiss Meditec Inc. (Dublin, CA, USA) Heidelberg Engineering (Heidelberg, Germany), and Optovue, Inc. (Fremont, CA, USA).

Appendix: Advanced Imaging for Glaucoma Study Group

The Advanced Imaging for Glaucoma (AIG) project is a bioengineering partnership (NIH 1 R01 EY013516) sponsored by the National Eye Institute to improve quantitative imaging technologies for glaucoma diagnosis and management. The AIG Study Group consists of the investigators and staff in the clinical study arm of the partnership and the supporting resource centers. The clinical study was active 2005-2013.

Principal Investigator: David Huang, MD, PhD[1]

Steering Committee: David Huang, MD, PhD (Chair)[1]; Brian Francis, MD[2]; David S. Greenfield, MD[3]; Richard K. Parrish II, MD[3] (2012-13); Joel S. Schuman, MD[4]; Rohit Varma, MD, MPH[5]

Clinical Centers:

Clinical Centers:
Bascom Palmer Eye Institute, Palm Beach, FL
Investigators: David S. Greenfield, MD*; Krishna S. Kishor, MD (2010-13); Carolyn D. Quinn, MD (2008-13)
Study Coordinators: Shawn Iverson, DO (2011-13); Nayara Kish, BS, CCRC (2010-12); Jose Rebimbas, BS, CCRC (2012-13); Debra Weiss, CRC (2003-10)
Doheny Eye Institute, Los Angeles, CA
Investigators: Brian Francis, MD*; Vikas Chopra, MD (2004-13); Rohit Varma, MD, MPH*[25]

Clinical Centers:
Study Coordinators: John Gil-Flamer, COT; Judith Linton, COA (2010-13); Sylvia Ramos, CCRP (2004-10)
University of Pittsburgh Medical Center Eye Center, Pittsburgh, PA
Investigators: Joel S. Schuman, MD*; Eiyass Albeiruti, MD (2009-13); Nils Loewen, MD (2012-13); Robert Noecker, MD (2005-2010)
Study Coordinators: Michael DeRosa, BS, BA (2012-13); Greg Owens, BA, CCRP (2010-13); Melessa Salay, BA (2010-13); Kristy Truman, COA (2010-13)

* Site principal investigator

Resource Centers:

Resource Centers:
Coordinating Center
David Huang, MD, PhD (Director); Janice Ladwig, COT, CCRP (2012-13), Michelle Montalto, BS (2010-12); Sylvia Ramos, CCRP (2004-10)
Advanced Imaging Analysis
Hiroshi Ishikawa, MD[4]; Larry Kagemann, MS[4] (2003-10); Mitra Sehi, PhD[3]; Ou Tan, PhD[1]; Yimin Wang, PhD[1] (2006-12); Gadi Wollstein, MD[4]
Database
Sharon Bi[6], MCIS (2006-13); Swati Chakraborty, MS (2003-09); Robert DiLaura, MBA, DBA[6] (2009-12); Bo Hu, PhD[6] (2012-13); John Sell (2003-06)
Disc Reading Center (2012-13)
Richard K. Parrish II, MD (Director); Eleonore Savatovsky, PhD
Doppler OCT Reading Center (2009-13)
Srinivas R. Sadda, MD (Director); Ranjith Konduru, MD (2009-12); Elnaz Rakhshan, MD (2011-12); Sowmya Srinivas, MBBS (2011-13)
Statistics
Ake T.H. Lu, PhD (2004-09); Xinbo Zhang, PhD1 (2009-13)

* Site principal investigator

[1] Casey Eye Institute, Oregon Health & Science University, Portland, OR

[2] Doheny Eye Institute, University of Southern California, Keck School of Medicine, Los Angeles, CA

[3] Bascom Palmer Eye Institute, University of Miami Miller School of Medicine, Miami, FL

[4] University of Pittsburgh Medical Center Eye Center, Swanson School of Engineering, University of Pittsburgh, Pittsburgh, PA

[5] University of Illinois-Chicago, Chicago, IL (after 2012)

[6] Cleveland Clinic, Cleveland, OH

1. Casey Eye Institute, Oregon Health & Science University, Portland, OR

2. Doheny Eye Institute, University of Southern California, Keck School of Medicine, Los Angeles, CA

3. Bascom Palmer Eye Institute, University of Miami Miller School of Medicine, Miami, FL

4. University of Pittsburgh Medical Center Eye Center, Swanson School of Engineering, University of Pittsburgh, Pittsburgh, PA

5. University of Illinois-Chicago, Chicago, IL (after 2012)

6. Cleveland Clinic, Cleveland, OH

Advanced Imaging for Glaucoma Study Group: Financial Interest Statements

Dr. Chopra received honoraria from Optovue, Inc. (Fremont, CA, USA). Dr. Greenfield receives research support from Optovue Inc. (Fremont, CA, USA), Carl Zeiss Meditec, Inc. (Dublin, CA, USA), and Heidelberg Engineering (Heidelberg, Germany). Drs. Huang and Schuman receive royalties for an optical coherence tomography patent owned and licensed by the Massachusetts Institute of Technology and Massachusetts Eye & Ear Infirmary to Carl Zeiss Meditec, Inc. (Dublin, CA, USA). Drs. Huang, Tan and Wang have a financial interest in Optovue, Inc. (Fremont, CA, USA), a company involved in the study. The nature of this financial interest and the design of the study have been reviewed by a committee at Oregon Health & Science University and a plan has been put into place to ensure this research study is not affected by the financial interest. Dr. Sadda has served as a consultant for Optos plc (Dunfermline, Scotland, UK), and Carl Zeiss Meditec, Inc. (Dublin, CA, USA) and has received research support from Optovue Inc. (Fremont, CA, USA), Optos plc (Dunfermline, Scotland, UK), and Carl Zeiss Meditec. Inc. (Dublin, CA, USA). Dr. Varma received research grants, honoraria and/or travel support from Carl Zeiss Meditec, Inc. (Dublin, CA, USA), Heidelberg Engineering (Heidelberg, Germany), and Optovue Inc. (Fremont, CA, USA).

Information

www.AIGStudy.net

Biography

Dr. Phuc (Phillip) Le graduated from the Massachusetts Institute of Technology with Bachelor's and Master's degrees in Engineering. He then matriculated at the University of Pennsylvania, earning an MD as well as a Ph.D. in Genetics. He completed his ophthalmology residency at the University of Southern California -Doheny Eye Institute, where he served an additional year as Assistant Chief of Service. He has recently completed a fellowship in medical retina at the University of Southern California.

References

1. Quigley HA, Broman AT. The number of people with glaucoma worldwide in 2010 and 2020. Br J Ophthalmol. Mar; 2006 90(3):262–267. [PubMed: 16488940]
2. Sommer A, Katz J, Quigley HA, et al. Clinically detectable nerve fiber atrophy precedes the onset of glaucomatous field loss. Arch Ophthalmol. Jan; 1991 109(1):77–83. [PubMed: 1987954]
3. Kass MA. The ocular hypertension treatment study. J Glaucoma. 1994; 3(2):97–100. Summer. [PubMed: 19920560]
4. Lin SC, Singh K, Jampel HD, et al. Optic nerve head and retinal nerve fiber layer analysis: a report by the American Academy of Ophthalmology. Ophthalmology. Oct; 2007 114(10):1937–1949. [PubMed: 17908595]
5. Townsend KA, Wollstein G, Schuman JS. Imaging of the retinal nerve fibre layer for glaucoma. Br J Ophthalmol. Feb; 2009 93(2):139–143. [PubMed: 19028735]
6. Vizzeri G, Kjaergaard SM, Rao HL, Zangwill LM. Role of imaging in glaucoma diagnosis and follow-up. Indian J Ophthalmol. Jan; 2011 59(Suppl):S59–68. [PubMed: 21150036]
7. Zangwill LM, Bowd C, Berry CC, et al. Discriminating between normal and glaucomatous eyes using the Heidelberg Retina Tomograph, GDx Nerve Fiber Analyzer, and Optical Coherence Tomograph. Arch Ophthalmol. Jul; 2001 119(7):985–993. [PubMed: 11448320]
8. Greaney MJ, Hoffman DC, Garway-Heath DF, Nakla M, Coleman AL, Caprioli J. Comparison of optic nerve imaging methods to distinguish normal eyes from those with glaucoma. Invest Ophthalmol Vis Sci. Jan; 2002 43(1):140–145. [PubMed: 11773024]
9. Medeiros FA, Zangwill LM, Bowd C, Weinreb RN. Comparison of the GDx VCC scanning laser polarimeter, HRT II confocal scanning laser ophthalmoscope, and stratus OCT optical coherence tomograph for the detection of glaucoma. Arch Ophthalmol. Jun; 2004 122(6):827–837. [PubMed: 15197057]
10. Kanamori A, Nagai-Kusuhara A, Escano MF, Maeda H, Nakamura M, Negi A. Comparison of confocal scanning laser ophthalmoscopy, scanning laser polarimetry and optical coherence tomography to discriminate ocular hypertension and glaucoma at an early stage. Graefes Arch Clin Exp Ophthalmol. Jan; 2006 244(1):58–68. [PubMed: 16044326]
11. Vessani RM, Moritz R, Batis L, Zagui RB, Bernardoni S, Susanna R. Comparison of quantitative imaging devices and subjective optic nerve head assessment by general ophthalmologists to differentiate normal from glaucomatous eyes. J Glaucoma. Mar; 2009 18(3):253–261. [PubMed: 19295383]
12. Bowd C, Zangwill LM, Weinreb RN. Association between scanning laser polarimetry measurements using variable corneal polarization compensation and visual field sensitivity in glaucomatous eyes. Arch Ophthalmol. Jul; 2003 121(7):961–966. [PubMed: 12860798]
13. Lisboa R, Paranhos A Jr. Weinreb RN, Zangwill LM, Leite MT, Medeiros FA. Comparison of different spectral domain OCT scanning protocols for diagnosing preperimetric glaucoma. Invest Ophthalmol Vis Sci. 2013; 54(5):3417–3425. [PubMed: 23532529]
14. Optic nerve head and retinal nerve fiber layer analysis. American Academy of Ophthalmology. Ophthalmology. Jul; 1999 106(7):1414–1424. [PubMed: 10406631]
15. Kass MA, Heuer DK, Higginbotham EJ, et al. The Ocular Hypertension Treatment Study: a randomized trial determines that topical ocular hypotensive medication delays or prevents the onset of primary open-angle glaucoma. Arch Ophthalmol. Jun; 2002 120(6):701–713. discussion 829-730. [PubMed: 12049574]
16. Fisher, RA. Statistical methods for research workers. Oliver and Boyd; Edinburgh, London: 1925.
17. Liang K-Y, Zeger SL. Longitudinal data analysis using generalized linear models. Biometrika. Apr 1; 1986 73(1):13–22. 1986.
18. Brusini P, Filacorda S. Enhanced Glaucoma Staging System (GSS 2) for classifying functional damage in glaucoma. J Glaucoma. Feb; 2006 15(1):40–46. [PubMed: 16378017]
19. Zangwill L, Berry CA, Garden VS, Weinreb RN. Reproducibility of retardation measurements with the nerve fiber analyzer II. J Glaucoma. Dec; 1997 6(6):384–389. [PubMed: 9407367]
20. Garas A, Toth M, Vargha P, Hollo G. Comparison of repeatability of retinal nerve fiber layer thickness measurement made using the RTVue Fourier-domain optical coherence tomograph and

the GDx scanning laser polarimeter with variable or enhanced corneal compensation. J Glaucoma. Aug; 2010 19(6):412–417. [PubMed: 19855292]

21. Sihota R, Gulati V, Agarwal HC, Saxena R, Sharma A, Pandey RM. Variables affecting test-retest variability of Heidelberg Retina Tomograph II stereometric parameters. J Glaucoma. Aug; 2002 11(4):321–328. [PubMed: 12169969]
22. Strouthidis NG, White ET, Owen VM, Ho TA, Hammond CJ, Garway-Heath DF. Factors affecting the test-retest variability of Heidelberg retina tomograph and Heidelberg retina tomograph II measurements. Br J Ophthalmol. Nov; 2005 89(11):1427–1432. [PubMed: 16234446]
23. Gordon MO, Kass MA. The Ocular Hypertension Treatment Study: design and baseline description of the participants. Arch Ophthalmol. May; 1999 117(5):573–583. [PubMed: 10326953]
24. Miglior S, Zeyen T, Pfeiffer N, Cunha-Vaz J, Torri V, Adamsons I. The European glaucoma prevention study design and baseline description of the participants. Ophthalmology. Sep; 2002 109(9):1612–1621. [PubMed: 12208707]
25. Zangwill LM, Weinreb RN, Berry CC, et al. Racial differences in optic disc topography: baseline results from the confocal scanning laser ophthalmoscopy ancillary study to the ocular hypertension treatment study. Arch Ophthalmol. Jan; 2004 122(1):22–28. [PubMed: 14718290]
26. Hoffmann EM, Miglior S, Zeyen T, et al. The Heidelberg retina tomograph ancillary study to the European glaucoma prevention study: study design and baseline factors. Acta Ophthalmol (Copenh). Dec; 2013 91(8):e612–619.
27. Sehi M, Guaqueta DC, Feuer WJ, Greenfield DS. Scanning laser polarimetry with variable and enhanced corneal compensation in normal and glaucomatous eyes. Am J Ophthalmol. Feb; 2007 143(2):272–279. [PubMed: 17157800]
28. Sehi M, Guaqueta DC, Greenfield DS. An enhancement module to improve the atypical birefringence pattern using scanning laser polarimetry with variable corneal compensation. Br J Ophthalmol. Jun; 2006 90(6):749–753. [PubMed: 16481378]
29. Bagga H, Greenfield DS, Feuer WJ. Quantitative assessment of atypical birefringence images using scanning laser polarimetry with variable corneal compensation. Am J Ophthalmol. Mar; 2005 139(3):437–446. [PubMed: 15767051]
30. Windisch BK, Harasymowycz PJ, See JL, et al. Comparison between confocal scanning laser tomography, scanning laser polarimetry and optical coherence tomography on the ability to detect localised retinal nerve fibre layer defects in glaucoma patients. Br J Ophthalmol. Feb; 2009 93(2): 225–230. [PubMed: 18765430]
31. Tan O, Li G, Lu AT, Varma R, Huang D. Mapping of macular substructures with optical coherence tomography for glaucoma diagnosis. Ophthalmology. Jun; 2008 115(6):949–956. [PubMed: 17981334]
32. Tan O, Chopra V, Lu AT, et al. Detection of macular ganglion cell loss in glaucoma by Fourier-domain optical coherence tomography. Ophthalmology. Dec; 2009 116(12):2305–2314. e2301–2302. [PubMed: 19744726]
33. Ishikawa H, Stein DM, Wollstein G, Beaton S, Fujimoto JG, Schuman JS. Macular segmentation with optical coherence tomography. Invest Ophthalmol Vis Sci. Jun; 2005 46(6):2012–2017. [PubMed: 15914617]
34. Leung CK, Yu M, Weinreb RN, et al. Retinal nerve fiber layer imaging with spectral-domain optical coherence tomography: a prospective analysis of age-related loss. Ophthalmology. Apr; 2012 119(4):731–737. [PubMed: 22264886]
35. Leung CK, Ye C, Weinreb RN, Yu M, Lai G, Lam DS. Impact of Age-related Change of Retinal Nerve Fiber Layer and Macular Thicknesses on Evaluation of Glaucoma Progression. Ophthalmology. Dec; 2013 120(12):2485–2492. [PubMed: 23993360]

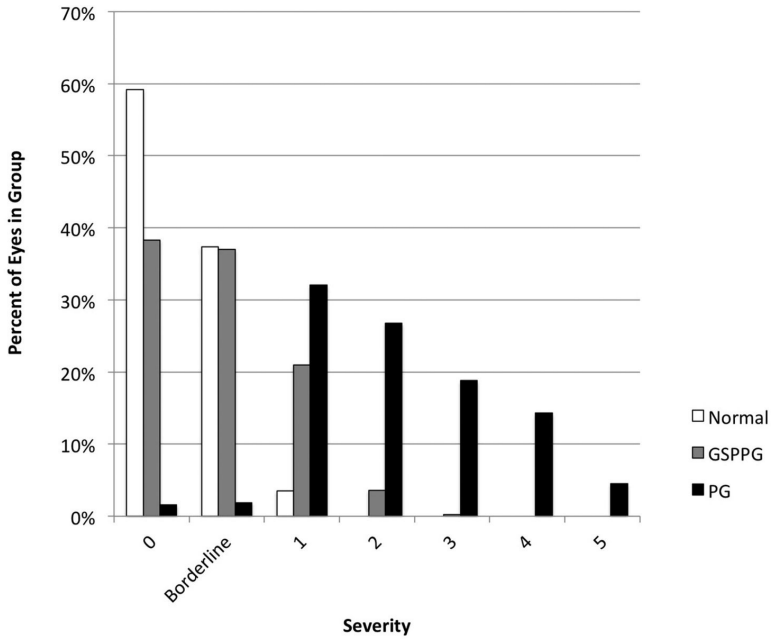

Figure 1.

Distribution of glaucoma severity at baseline for eyes in the Normal, Glaucoma Suspect/ Preperimetric Glaucoma, and Perimetric Glaucoma groups of the Advanced Imaging for Glaucoma Study. Severity of glauomca based on the enhanced Glaucoma Staging System 2 scale[18] GSPPG = Glaucoma Suspect/Preperimetric Glaucoma. PG = Perimetric Glaucoma.

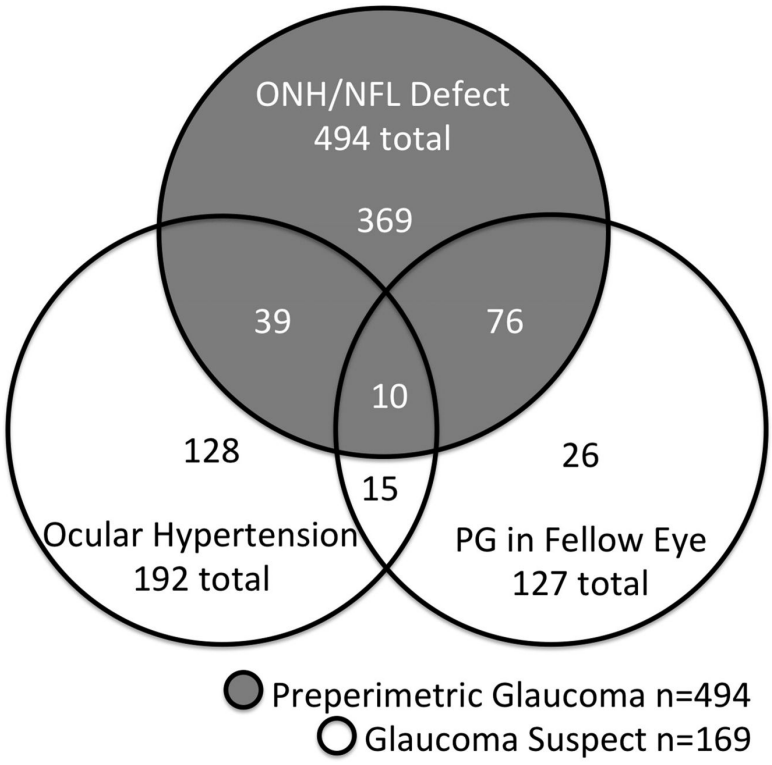

Figure 2.

Venn diagram of the characteristics of eyes comprising the Glaucoma Suspect/Preperimetric Glaucoma group of the Advanced Imaging for Glaucoma Study. ONH = Optic Nerve Head. NFL = Nerve Fiber Layer.

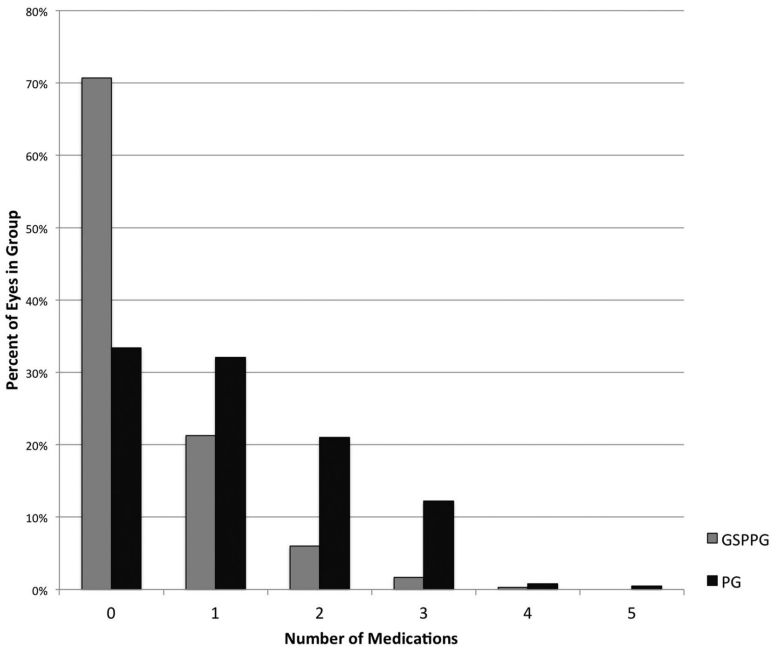

Figure 3.

Distribution of the number of topical intraocular pressure-lowering medications in use at baseline for eyes in the Glaucoma Suspect/Preperimetric Glaucoma and Perimetric Glaucoma groups of the Advanced Imaging for Glaucoma Study.

Table 1

Descriptive Statistics of Participants at Baseline in the Advanced Imaging for Glaucoma Study, Divided by Clinical Center

	UP	UM	USC	Overall
Number of Participants				
Normal	56	49	40	145
GSPPG	158	104	132	394
PG	74	75	100	249
Total	288	228	272	788
Number of Eyes				
Normal	111	98	80	289
GSPPG	278	171	214	663
PG	110	117	150	377
Total	499	386	444	1329
Age±SD (years)				
Normal	53.1±9.0	59.2±10.2	56.8±8.7	56.2±9.7
GSPPG	60.1±9.8	63.9±9.3	58.4±8.8	60.5±9.5
PG	62.5±9.6	64.8±8.8	59.6±9.2	62.0±9.4
Gender: Female (%)				
Normal	75	55	63	64.8
GSPPG	66	63	52	60.7
PG	66	64	51	59.4
Race: African American (%)				
Normal	9	4	8	6.9
GSPPG	17	10	8	11.9
PG	14	8	10	10.4

UP = University of Pittsburgh; UM = University of Miami; USC = University of Southern California; GSPPG = glaucoma suspect/preperimetric glaucoma; PG = perimetric glaucoma; SD = standard deviation

Table 2

Clinical Characteristics of Eyes at Baseline Within the Normal, Glaucoma Suspect/Preperimetric Glaucoma, and Perimetric Glaucoma Groups of the Advanced Imaging for Glaucoma Study.

	Normal	GSPPG	p[a] (Normal v. GSPPG)	PG	p[a] (Normal v. PG)
Axial Length (mm)	23.8 ± 1.0	24.2 ± 1.3	<0.0001	24.3 ± 1.3	<0.0001
MR Sphere (D)	−0.71± 1.98	−1.21 ± 2.34	0.026	−0.96 ± 2.47	0.069
MR Cylinder (D)	0.54 ± 0.72	0.61 ± 0.79	0.25	0.65 ± 0.74	0.16
CCT (Mm)	562 ± 32	557 ± 39	0.0103	545 ± 37	0.0002
IOP (mmHg)	14.8 ± 2.8	16.4 ± 4.0	<0.0001	14.9 ± 4.1	0.016
VF MD (dB)	0.01 ± 0.93	−0.61 ± 1.47	<0.0001	−5.01 ± 4.52	<0.0001
VF PSD (dB)	1.44 ± 0.20	1.68 ± 0.42	<0.0001	5.76 ± 4.02	<0.0001
Visual Field Index	99.5 ± 0.6	98.8 ± 1.8	<0.0001	87.9 ± 13.6	<0.0001
Vertical CDR	0.34 ± 0.19	0.52 ± 0.24	<0.0001	0.70 ± 0.23	<0.0001
Horizontal CDR	0.33 ± 0.18	0.49 ± 0.23	<0.0001	0.65 ± 0.22	<0.0001

Values are means ± standard deviations; GSPPG = glaucoma suspect/preperimetric glaucoma; PG = perimetric glaucoma; MR = manifest refraction; D = diopter; CCT = central corneal thickness; IOP = intraocular pressure, VF = visual field; MD = mean deviation; PSD = pattern standard deviation; CDR = cup-to-disc ratio by clinical ophthalmoscopy

[a] p-value by Generalized Estimating Equation.

Table 3

Imaging Parameters at Baseline in the Normal, Glaucoma Suspect/Preperimetric Glaucoma, and Perimetric Glaucoma Groups of the Advanced Imaging for Glaucoma Study.

Variable	Normal	GSPPG	p[a] (Normal v. GSPPG)	PG	p[a] (Normal v. PG)
TD-OCT					
Overall NFL (μm)	99.2±9.9	92.8±13.2	<0.0001	77.1±15.5	<0.0001
Superior NFL (μm)	120.2±15.2	112.1±20.5	<0.0001	92.4±23.3	<0.0001
Inferior NFL (μm)	128.4±15.8	117.8±19.7	<0.0001	91.6±25.4	<0.0001
Nasal NFL (μm)	79.1±17.2	72.6±17.1	<0.0001	64.3±16.3	<0.0001
Temp. RNFL (μm)	69.7±13.7	68.3±14.8	0.13	60.0±16.7	<0.0001
FD-OCT					
Overall NFL (μm)	99.6±8.0	93.5±10.1	<0.0001	81.3±12.2	<0.0001
Superior NFL (μm)	121.0±11.0	113.8±14.7	<0.0001	97.6±18.7	<0.0001
Inferior NFL (μm)	123.6±12.1	114.6±15.0	<0.0001	94.2±19.2	<0.0001
Nasal NFL (μm)	79.6±10.8	74.2±10.4	<0.0001	67.8±11.7	<0.0001
Temp. NFL (μm)	74.3±7.9	71.7±9.7	0.0011	65.7±11.3	<0.0001
Overall GCC (μm)	97.3±6.9	92.9±8.1	<0.0001	83.5±10.8	<0.0001
Superior GCC (μm)	96.8±6.9	92.8±8.3	<0.0001	85.7±11.4	<0.0001
Inferior GCC (μm)	97.8±7.2	93.1±8.6	<0.0001	81.4±12.9	<0.0001
cSLO					
Overall NFL (mm)	0.26±0.07	0.24±0.07	<0.0001	0.19±0.08	<0.0001
Rim Area (mm^2)	1.41±0.40	1.32±0.34	0.0009	1.08±0.34	<0.0001
SLP					
Overall NFL (μm)	53.9±4.8	52.4±7.5	0.0008	45.5±7.6	<0.0001
Superior NFL (μm)	66.6±7.4	63.9±8.8	<0.0001	55.7±11.3	<0.0001
Inferior NFL (μm)	67.01±7.2	64.9±8.6	<0.0001	55.3±12.9	<0.0001

Values are means±standard deviations; GSPPG = glaucoma suspect/preperimetric glaucoma; PG = perimetric glaucoma; TD-OCT = time-domain optical coherence tomography; FD-OCT = Fourier-domain optical coherence tomography; cSLO = confocal scanning laser ophthalmoscopy; SLP = scanning laser polarimetry; NFL = peripapillary retinal nerve fiber layer thickness; GCC = macular ganglion cell complex thickness; Temp. = temporal.

[a] p-value by Generalized Estimating Equation.

Table 4

Imaging Parameters at Baseline in the Normal, Glaucoma Suspect/Preperimetric Glaucoma, and Perimetric Glaucoma Groups of the Advanced Imaging for Glaucoma Study, Divided by Clinical Center

	UP	UM	USC	p[a]
Normal Group				
TD-OCT NFL (μm)	99.9±10.1	97.9±9.1	99.8±10.6	0.53
FD-OCT NFL (μm)	98.6±8.3	99.2±8.5	101.8±6.3	0.18
FD-OCT GCC (μm)	97.9±7.4	95.8±6.8	98.3±6.1	0.19
cSLO NFL (μm)	0.27±0.06	0.25±0.07	0.27±0.07	0.06
cSLO Rim Area (mm^2)	1.34±0.29	1.32±0.42	1.60±0.44	0.0003
SLP NFL (μm)	55.2±4.8	51.7±4.2	54.6±4.5	0.0002
GSPPG Group				
TD-OCT NFL (μm)	94.1±13.5	91.1±12.4	92.5±13.4	0.25
FD-OCT NFL (μm)	94.3±9.6	93.3±9.6	92.8±11.2	0.77
FD-OCT GCC (μm)	93.7±8.5	91.4±7.2	93.3±8.2	0.044
cSLO NFL (μm)	0.24±0.07	0.24±0.07	0.22±0.08	0.063
cSLO Rim Area (mm^2)	1.33±0.31	1.25±0.33	1.36±0.37	0.043
SLP NFL (μm)	53.6±5.4	51.1±10.8	51.5±5.9	0.038
PG Group				
TD-OCT NFL (μm)	80.9±14.3	73.6±16.4	77.1±15.2	0.02
FD-OCT NFL (μm)	85.3±11.1	79.5±13.8	79.9±10.6	0.018
FD-OCT GCC (μm)	87.0±11.4	80.8±10.6	83.6±9.7	0.003
cSLO NFL (mm)	0.21±0.09	0.18±0.07	0.19±0.07	0.078
cSLO Rim Area (mm^2)	1.17±0.35	1.00±0.28	1.08±0.36	0.017
SLP NFL (μm)	49.0±7.1	41.9±6.8	45.1±7.5	<0.0001

Values are means±standard deviations; UP = University of Pittsburgh; UM = University of Miami; USC = University of Southern California; GSPPG = glaucoma suspect/preperimetric glaucoma; PG = perimetric glaucoma; TD-OCT = time-domain optical coherence tomography; FD-OCT = Fourier-domain optical coherence tomography; cSLO = confocal scanning laser ophthalmoscopy; SLP = scanning laser polarimetry; NFL = peripapillary retinal nerve fiber layer thickness; GCC = macular ganglion cell complex thickness.

[a] p-value calculated by mixed models;

Table 5

Repeatability of Imaging Parameters at Baseline in the Normal, Glaucoma Suspect/Preperimetric Glaucoma, and Perimetric Glaucoma Groups of the Advanced Imaging for Glaucoma Study, Divided by Clinical Center

	Coefficient of Variation (%)				Overall ICC
	UP	UM	USC	Overall	
Normal Group					
TD-OCT NFL	2.1	1.9	2.1	2.0	0.96
FD-OCT NFL	1.3	1.5	1.1	1.3	0.97
FD-OCT GCC	1.1	1.2	1.0	1.1	0.98
cSLO NFL	6.3	6.2	7.4	6.6	0.93
cSLO Rim Area	3.7	2.3	5.5	4.2	0.98
SLP NFL	2.7	1.9	3.1	2.6	0.92
GSPPG Group					
TD-OCT NFL	2.7	2.4	2.3	2.5	0.97
FD-OCT NFL	1.4	1.6	1.4	1.5	0.98
FD-OCT GCC	1.3	1.5	1.1	1.3	0.98
cSLO NFL	10.0	9.5	11.0	10.0	0.89
cSLO Rim Area	6.3	5.7	6.3	6.2	0.94
SLP NFL	3.5	2.7	3.3	3.2	0.92
PG Group					
TD-OCT NFL	3.1	2.7	2.8	2.9	0.98
FD-OCT NFL	1.6	1.6	1.4	1.5	0.99
FD-OCT GCC	1.4	1.5	1.2	1.4	0.99
cSLO NFL	13.0	14.0	15.0	14.0	0.88
cSLO Rim Area	8.1	6.0	8.1	7.6	0.94
SLP NFL	4.3	5.0	4.4	4.5	0.93

ICC = intraclass correlation coefficient; UP = University of Pittsburgh; UM = University of Miami; USC = University of Southern California; GSPPG = glaucoma suspect/preperimetric glaucoma; PG = perimetric glaucoma; TD-OCT = time-domain optical coherence tomography; FD-OCT = Fourier-domain optical coherence tomography; cSLO = confocal scanning laser ophthalmoscopy; SLP = scanning laser polarimetry; NFL = peripapillary retinal nerve fiber layer thickness; GCC = macular ganglion cell complex thickness.

Table 6

Mixed-Effect Model Analysis of Diagnostic Group, Inter-Site, Inter-Participant, and Inter-Eye Variables for Imaging Parameters of the Advanced Imaging for Glaucoma Study.

	Fixed Effects		Random Variations		
	GSPPG	PG	Inter-Site	Inter-Participant	Left-Right Eye
TD-OCT NFL (μm)	−7.7	−19.9	1.9	11.4	6.9
FD-OCT NFL (μm)	−6.9	−16.5	1.3	8.9	5.3
FD-OCT GCC (μm)	−4.9	−12.7	1.7	7.2	4.8
cSLO NFL (mm)	−0.03	−0.06	0.007	0.05	0.05
cSLO Rim Area (mm^2)	−0.12	−0.29	0.064	0.29	0.19
SLP NFL (μm)	−2.1	−7.4	1.8	6.1	4.0

GSPPG = glaucoma suspect/preperimetric glaucoma; PG = perimetric glaucoma; TD-OCT = time-domain optical coherence tomography; FD-OCT = Fourier-domain optical coherence tomography; cSLO = confocal scanning laser ophthalmoscopy; SLP = scanning laser polarimetry; NFL = peripapillary retinal nerve fiber layer thickness; GCC = macular ganglion cell complex thickness.